LA-UR-19-28330
Approved for public release; distribution is unlimited.

Title: Spectroscopy and solubility of U(IV) in dilute to concentrated NaCl solutions in the presence of EDTA at pHm 1-11

Author(s): Reed, Donald T.
Yalcintas, Ezgi
almtaier, Marcus
Gaona, Xavi
Richmann, Michael K
Dardenne, Kathy

Intended for: Environmental Science & Technology

Issued: 2019-08-21 (Rev.1) (Draft)

Spectroscopy and solubility of U(IV) in dilute to concentrated NaCl solutions in the presence of EDTA at pH_m 1-11

Ezgi Yalçıntaş[a], Xavier Gaona[b], Michael K. Richmann[a], Kathy Dardenne[b], Marcus Altmaier[b], Donald T. Reed[a]

[a]*Los Alamos National Laboratory, 88220, Carlsbad, USA*

[b]*Institute for Nuclear Waste Disposal, Karlsruhe Institute of Technology, PO Box 3640, 76021 Karlsruhe, Germany*

Abstract

The effects of EDTA on U(IV) aquatic chemistry were investigated by a combination of spectroscopy and solubility experiments in NaCl solutions. Spectroscopic measurements were performed with $1 \leq pH_m \leq 6.5$, 10^{-4} M $\leq$ [EDTA] $\leq$ 0.01 M and $0.2 \leq$ [U(IV)] : [EDTA] ≤ 10. These results show the formation of a 1:1 UEDTA(aq) complex with four isosbestic points at low pH. Spectroscopic changes at pH > 2.5 point toward the formation of monomeric $UEDTA(OH)_x^{x-}$ complexes. Solubility experiments with UO_2(s) were performed under reducing conditions ($pe + pH_m \leq 6.5$) at constant ionic strength I = 0.5 and 5.0 M NaCl at pH_m = 4–11. A significant increase in solubility was noted when compared to EDTA-free systems. This, combined with the slope analysis of the solubility data, cannot be explained with existing chemical and thermodynamic models and supports the formation of several $UEDTA(OH)_x^{x-}$ complexes. The spectroscopic and solubility results collectively point to the important role that EDTA has in defining the speciation and solubility of U(IV) species, and by analogy all actinide(IV) species, under environmentally relevant near-neutral to moderately high pH conditions. These results also point to the need to develop thermodynamic and activity models that describe this speciation in repository and subsurface contaminant applications.

Keywords: uranium(IV), EDTA, UV–Vis–NIR, solubility, XANES, brine

1 Introduction

Uranium is a key constituent of nuclear waste, is a common subsurface contaminant associated with nuclear fuel processing and uranium mining activities, and is also found naturally in near-surface groundwater. EDTA is a widely used strong complexant used in nuclear processing and decommissioning/decontamination activities. In the latter case, it is often co-disposed with uranium and other actinides.[1-4] This issue has particular relevance to the long-term performance of transuranic repository concepts in salt (e.g., WIPP) repository concepts,[1] as well as many near-surface DOE-site contamination problems where uranium and EDTA are known to co-exist.[2]

Uranium typically comprises the largest actinide inventory in treated transuranic and high-level radioactive waste and is the main component of spent fuel. Two main oxidation states define its environmental chemistry: U(VI) is the most stable oxidation state of uranium under sub-oxic and oxidizing conditions, exhibits amphoteric solubility behavior, and is generally the oxidation state most associated with high mobility scenarios in near-surface contamination. U(IV), in contrast, predominates in anoxic strongly-reducing environments and forms sparingly soluble UO_2(s) phases in the absence of complexing ligands. The +IV oxidation state, in broader terms, is also a key actinide oxidation state for other environmentally-important multivalent actinides such as plutonium and neptunium.

EDTA, when present in the environment, is not readily biodegradable and tends to form relatively stable and mobile complexes with actinides. Its importance in potentially mobilizing actinides in the subsurface was raised by others.[3-7] The interaction of EDTA with multivalent actinides, such as uranium, can also impact its oxidation state by preferential solubilization and redox mechanisms. These effects, although not well studied, would likely depend on pH, ligand/metal ratio, radiolysis and the initial oxidation state.

The complexation behavior of U(IV) with EDTA was initially[8-10] investigated potentiometrically and spectroscopically in the 50s and 60s. The 1:1 complex UEDTA(aq) is well stablished and is the only U(IV)-EDTA complex selected in the OECD / Nuclear Energy Agency Thermochemical Database (NEA–TDB).[11] The formation of additional complexes were proposed in these earlier studies[10, 12]: $UEDTA(OH)^{-}$, $(UEDTAOH)_2^{2-}$, $UEDTA(OH)_2^{2-}$, $U_2H_2EDTA_3^{2-}$, $U_2HEDTA_3^{3-}$, $U_2EDTA_3^{4-}$, $(UOH)_2EDTA_3^{4-}$, and U_2EDTA^{4+}. These species are predicted to form under varying experimental conditions as a function of pH, [EDTA], or U concentration. None of these ternary or polynuclear species were selected by the NEA–TDB due to the scarcity or unreliability of the experimental data, although the probable existence of the hydrolyzed UEDTA(aq) species was acknowledged.

There are in fact very few experimental studies that focused on U(IV)-EDTA complexes, especially at the more environmentally-relevant higher-pH range, despite their potential importance in both nuclear waste disposal concepts and near-surface contaminated sites. In this study, we revisited the complexation behavior of U(IV) with EDTA in a more systematic and comprehensive way as a function $[EDTA]_{tot}$, pH, and complex concentration by UV–Vis–NIR spectroscopy. This was coupled with a

first-time study of the effects of EDTA on the long-term solubility and redox stability of UO_2(s) under reducing conditions that covered acidic to alkaline pH, and dilute to concentrated NaCl solutions.

2 Experimental

2.1 Chemicals

All sample preparation and handling were performed in an inert nitrogen glove box at T = (22 ± 2) °C (MBraun recirculating, < 0.1 ppm O_2). All solutions were prepared with purified water (Barnstead, Gen Pure) and purged with N_2 for two hours before use to minimize O_2 and CO_2 in solution. $SnCl_2$ (Sigma-Aldrich anhydrous powder 99.99% trace metals), Na_4EDTA (Sigma-Aldrich 99%+), NaCl (Fisher certified ACS), HCl (Fisher, Optima 32-35%), NaOH (Acros 50%), HNO_3 (Fisher, Optima 67-70%), $HClO_4$ (Fisher, Trace metal 67-71%) and NIST-traceable pH buffers (Fisher certified) were used in the experiments.

The uranium stock solution was an aqueous U(IV) chloride solution that was prepared by dissolution of UCl_4(s) (International Bioanalytical Industries, U-238 isotope) in 2.0 M HCl in an anoxic/nitrogen glovebox. The initial oxidation state purity was confirmed by UV–Vis–NIR spectroscopy to be greater than 95% and was stable for periods of months when kept sealed in the anoxic glovebox. Uranium (VI) stock was prepared by dissolving U_3O_8 formed by stepwise heating $UO_2(NO_3)_2 \cdot 6H_2O$ (SPECTRAUM) at 650˚C[13] and dissolved in 0.1 M HCl in air. This was essentially 100% oxidation state purity and verified spectroscopically.

2.2 pH and E_h measurements

The hydrogen ion concentration (pH_m = –log [H^+], in molal units) was determined according to $pH_m = pH_{exp} + A_m$ as described previously in the literature,[14] where pH_{exp} is the measured pH value and A_m is the empirical correction factor entailing the liquid junction potential of the electrode and the activity coefficient of H^+. A_m values used in the present study were –0.01 and 0.92 for 0.5 and 5.0 M NaCl, respectively.[14]

Redox potentials were measured using Pt combination electrodes with Ag/AgCl reference system (Mettler Toledo) following the protocol previously described in the literature.[15, 16] The measured redox potentials were converted to the apparent electron activity (pe = −log a_{e^-}), according to the following equation: pe = 16.9 E_h (V). Solubility data as a function of the E_h (converted to pe) and pH_m values were plotted in the U *Pourbaix* diagram using the thermodynamic data summarized in Table S1 and Table S2 in the Supporting Information and the code Medusa developed by Puigdomènech, 1983.[17]

2.3 Sample preparation and characterization

The complexation behavior of U(IV) with EDTA was investigated by oversaturation and undersaturation approaches. Background electrolyte solutions were prepared with EDTA at constant ionic strengths of I = 0.5 and 5.0 M $Na_xH_{4-x}EDTA$–NaCl–HCl–NaOH. Oversaturation batch samples were prepared as a function of: (1) $[EDTA]_{tot} = 2 \cdot 10^{-4}$ M – $1 \cdot 10^{-2}$ M at $pH_m = 1$ in 0.5 M NaCl at constant [U(IV)] = 10^{-3} M , (2) pH_m = 1- 5.8 at constant [U]:$[EDTA]_{tot}$ = 1:8 with [U(IV)] = 10^{-3} M, (3) [U(IV)] = $1.4 \cdot 10^{-4}$ M – $1.3 \cdot 10^{-3}$ M at constant [U]:$[EDTA]_{tot}$ = 1:10 at pH_m = 4, and (4) [U(VI)] = 10^{-3} M at constant [U]:$[EDTA]_{tot}$ = 1:10 at pH_m = 3.5-4 . Undersaturation batch experiments were performed starting with UO_2(s) at I = 0.5 (1) and 5.0 M (2). The solid phase was precipitated by adding UCl_4(aq) in a solution with 5 mM Sn(II) at $pH_m > 13$ to avoid oxidation during the precipitation procedure. The precipitate was aged in the mother liquor for about 2 days and confirmed by XRD (Figure S1, supporting information) as crystalline-like UO_2(s) prior to use in the solubility experiments. About 3 mg of U(IV) solid phase were washed with 1 mL of water and added to 20 mL of the same matrix solution in 50 mL polypropylene vials. pH values were adjusted with HCl-NaCl and NaOH-NaCl at identical ionic strengths. 2 mM Sn(II) was used to maintain reducing conditions in each independent batch in oversaturation (2-3) and undersaturation (1-2) experiments. Note that the ratio [U(IV)]:$[EDTA]_{tot}$ was selected to allow for an excess of free EDTA even in the presence of the Sn(II) added for redox stability. Experimental conditions used in the present study are summarized in Table 1.

All samples from oversaturation experiments and selected samples from undersaturation experiments (see Table 1) were characterized by UV–Vis–NIR. Absorption spectra were collected in the wavelength range $350 \leq \lambda$ [nm] ≤ 800 using a Cary 5000 (Varian) UV–Vis–NIR spectrometer and gas-tight cuvettes. The samples were analysed unfiltered and centrifuged through a 3 or 10 kD filter prior to UV-Vis-NIR measurements. Spectra were recorded with a 0.2 nm data interval, a scan rate of 60 nm·min^{-1} and a bandpass of 0.6 nm in double beam mode. Typically, two or three absorption spectra were collected sequentially for each sample at room temperature to confirm that they were stable with respect to oxidation state and temperature drift (usually ~ 2-3 °C) from their temperature in the glovebox.

Uranium concentrations were determined by ICP–MS (inductively coupled plasma mass spectrometry, Agilent 7900). A fraction of the supernatant (100 µL) of each sample was centrifuged in the nitrogen glovebox for 2–10 minutes with 10 kD filters (2–3 nm cut-off Nanosep® centrifuge tubes, Pall Life Sciences) to separate colloids or suspended solid particles. Aliquots of the original samples were diluted up to 1:1000 times with 2% HNO_3 before ICP–MS measurements. Blank measurements resulted in 0.0001–0.0006 ppb of U-238, which corresponded to effective detection limits of ≈ 10^{-9} to ≈ 10^{-11} mol·L^{-1} in the original solution depending on sample dilutions made to account for the salt content.

X–ray diffraction (XRD) analysis was performed for the initial U(IV) solid phase and selected solid phases after reaching equilibrium in the EDTA-NaCl systems. Diffractograms were collected with a

Bruker AXS D8 Advance X-ray powder diffractometer at $5 \leq 2\theta \leq 100°$ with incremental steps of 0.02° and a measurement time of 8 seconds per step.

Table 1 Experimental conditions used in the U(IV)-EDTA complexation and solubility experiments.

Sets	$[U(IV)]_{ini}$ (M)	$[EDTA]_{tot}$ (M)	pH_m[d]	Ionic strength (M)[e]	Type of experiment
Oversat. (1)	0.001 M	0	~1.0	0.5	spect.
	0.001 M	0.0002	~1.0	0.5	spect.
	0.001 M	0.0005	~1.0	0.5	spect.
	0.001 M	0.001	~1.0	0.5	spect.
	0.001 M	0.01	~1.0	0.5	spect.
Oversat. (2)[a]	0.0013 M[c]	0.01	~0.3	0.5	spect., XANES
	0.0012 M	0.01	1.0	0.5	spect.
	0.0012 M	0.01	2.5	0.5	spect.
	0.0012 M	0.01	3.0	0.5	spect.
	0.0012 M	0.01	3.5	0.5	spect.
	0.0012 M	0.01	4.0	0.5	spect.
	0.0013 M[c]	0.01	4.3	0.5	spect., XANES
	0.0012 M	0.01	4.8	0.5	spect.
	0.0012 M	0.01	5.8	0.5	spect.
	0.0013 M[c]	0.01	6.5	0.5	spect., XANES
Oversat. (3)[a]	0.00014 M	0.0014	4	0.5	spect.
	0.0006 M	0.006	4	0.5	spect.
	0.001 M	0.01	4	0.5	spect.
	0.0013 M	0.013	4	0.5	spect.
Oversat. (4)[b]	0.001 M	0.01	3.5	0.5	sol., XRD, spect.
	0.001 M[c]	0.01	4.1	0.5	sol., XRD, spect., XANES
Undersat.(1)[a]	~3 mg UO_2(s)	0.01	3.9	0.5	sol., spect.
	~3 mg UO_2(s)	0.01	6.0	0.5	sol., spect.
	~3 mg UO_2(s)	0.01	7.2	0.5	sol.
	~3 mg UO_2(s)	0.01	7.6	0.5	sol.
	~3 mg UO_2(s)	0.01	8.0	0.5	sol.
	~3 mg UO_2(s)	0.01	8.5	0.5	sol.
	~3 mg UO_2(s)	0.01	8.6	0.5	sol., XRD
	~3 mg UO_2(s)	0.01	9.6	0.5	sol.
	~3 mg UO_2(s)	0.01	10.9	0.5	sol.
Undersat.(2)[a]	~3 mg UO_2(s)	0.01	5.8	5.0	sol., spect.
	~3 mg UO_2(s)	0.01	6.3	5.0	sol., spect.
	~3 mg UO_2(s)	0.01	7.7	5.0	sol.
	~3 mg UO_2(s)	0.01	8.0	5.0	sol.
	~3 mg UO_2(s)	0.01	8.8	5.0	sol.
	~3 mg UO_2(s)	0.01	9.0	5.0	sol., XRD
	~3 mg UO_2(s)[c]	0.01	9.0	5.0	sol., XANES
	~3 mg UO_2(s)	0.01	9.7	5.0	sol.
	~3 mg UO_2(s)	0.01	11.0	5.0	sol.

[a]These samples are prepared with 2 mM Sn(II) to maintain reducing conditions.
[b]These samples are prepared with U(VI)(aq).
[c]These samples are prepared at KIT-INE laboratories.
[d] ± 0.05.
[e]Total ionic strength defined by $Na_xH_{4-x}EDTA$–NaCl–HCl–NaOH.
spect.: spectroscopic measurements, UV–Vis–NIR; sol.: solubility measurements

2.4 XANES analysis

Uranium L_{III}-edge X-ray absorption near-edge structure (XANES) spectra were recorded at the INE-Beamline at the KIT synchrotron light source, KIT Campus North, in Karlsruhe, Germany.[18, 19] Selected experiments (5 samples, see Tables 1 and 2) were reproduced in KIT-INE laboratories and analyzed to determine the redox state of U (within the detection limit of the technique, ≤ 10%). All samples prepared were equilibrated for 6 months before the XANES measurements. The spectra obtained for these samples were compared with the reference spectra of UO_2(s), $UO_3 \cdot 2H_2O$(cr) and $Na_2U_2O_7 \cdot H_2O$(cr) references measured at the same beamline and same set-up.

For these XANES analyses, care was taken to preserve the oxidation state of the uranium phase. In all cases, the uranium phase was transferred as an approximately 300 µL slurry to a 400 µL polyethylene vial under an Ar atmosphere. This was subsequently centrifuged to separate the dissolved and precipitated components. XANES analyses were performed on the aqueous and/or solid phase depending on the analytical objective. These vials were mounted in a gas-tight cell with Kapton® film windows inside the Ar-glovebox and transported intact to KARA, where the cell was connected under a continuous flow of Ar before and during the measurements. This set-up has been proven to be particularly appropriate for the characterization of redox-sensitive samples (*e.g.* Pu(III), U(IV), Np(IV), Tc(IV), Se(-II))[20-24] without the need to establish cryogenic conditions. It also permits the investigation of the aqueous part of the sample in contact with the solid. All measurements were made within a few hours after sample preparation.

The XANES spectra, (Uranium L_{III}-edge at 17166 eV), typically 2–6 replicates per sample, were collected at room temperature. The INE-Beamline is equipped with a Ge(422) double crystal monochromator (DCM) coupled with a collimating and a focusing Rh coated mirrors before and after the DCM, respectively. The DCM-crystals were detuned at 70%. The beam spotsize on the sample was less than 1mm in diameter and the energy calibration was performed by assigning the energy of 17038 eV to the first inflection point of the K-edge absorption spectrum of the Y metal foil reference. The incident and transmitted beam intensities were measured by argon-filled ionization chambers. XANES data reduction and analysis were performed with the ATHENA software of the Demeter 0.9.26 package following standard procedures.[25]

3 Results and discussion

3.1 Absorption spectra of UEDTA in the acidic to neutral pH range

Absorption spectra of U(IV) were obtained under acidic conditions at variable $[EDTA]_{tot}$ to establish spectral trends due to the formation of U(IV)-EDTA complexes. These spectra are shown in Figure 1a for $[EDTA]_{tot} = 2 \cdot 10^{-4}$ M – $1 \cdot 10^{-2}$ M, $[U(IV)] = 1 \cdot 10^{-3}$ M, at $pH_m = 1$, and in 0.5 M NaCl after 1 day of

contact time. The addition of EDTA instantly forms a strong complex with U(IV) and no further spectral changes were observed over the course of the experiments. In the absence of EDTA, the spectra (λ_{max} at 648 nm) obtained were in excellent agreement with the published data for the U^{4+} aqua ion.[20, 26] It was also confirmed that there was no difference between the absorption spectra of U^{4+} in 0.5 HCl and 1.0 M $HClO_4$, which indicated that U(IV)-Cl complexes can be neglected for this chloride concentration. The absorption band undergoes a red-shift with increasing EDTA concentration and showed four isosbestic points at 442 ± 0.2, 499 ± 0.2, 555.6 ± 0.2 and 653.8 ± 0.2 nm. These isosbestic points confirm the presence of only two species for the investigated pH and [U(IV)]:$[EDTA]_{tot}$ ratios. The maximum of the absorption band shifts to 655.2 ± 0.2 nm at $[EDTA]_{tot} = 10^{-3}$ M and no further shift is observed even in $[EDTA]_{tot} = 10^{-2}$ M.

The spectral results reported in this study, although a much broader wavelength range was covered, agree with previously reported absorption spectra at $560 < \lambda$ [nm] < 720 for UEDTA(aq).[10] These spectral features support the formation of a 1:1 UEDTA(aq) complex in the acidic pH region, as reported in the literature[8-10] and predicted with thermodynamic calculations using selected data in the NEA–TDB.[11] The molar extinction coefficient for the UEDTA(aq) complex was quantified at $pH_m \approx 1$ as $\varepsilon = (36 \pm 5)$ $L \cdot mol^{-1} \cdot cm^{-1}$ at $\lambda = 655.2$ nm (1 cm path length) and had a Beer-Lambert dependency. The formation of polynuclear or oligomeric species ($U_2H_2EDTA_3^{2-}$, $U_2HEDTA_3^{3-}$) reported by Ermolaev and Krot[12] that formed with excess U or EDTA were not observed for the range of conditions investigated in the present study.

The effect of pH on the absorption spectra of U(IV) in the EDTA system is shown in Figure 1b: [U(IV)]:$[EDTA]_{tot}$ = 1:8 and 0.5 M NaCl. All samples were monitored for up to 110 days of contact time and the spectra were taken after 3 kD and 10 kD ultrafiltration to eliminate the presence of colloidal species larger than 2-3 nm. No notable changes were observed in the UEDTA(aq) absorption spectrum until $pH_m = 2.5$, where the onset of hydrolysis led to changes in the spectra.

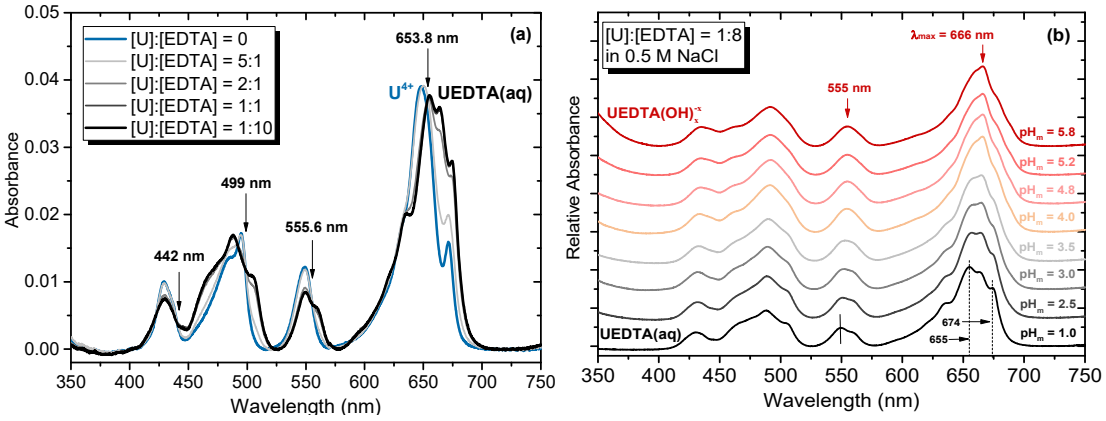

Figure 1 Absorption spectra of U(IV) (a) as a function of $[EDTA]_{tot}$ at $pH_m = 1$ in 0.5 M NaCl, (b) as a function of pH_m in 0.5 M NaCl at a fixed $[EDTA]_{tot}$.

The spectral shifts noted were relatively complex and not the same for each absorption band. A λ_{max} shift from 655.2 ± 0.2 to 666 ± 0.2 nm with increasing pH_m (up to 5.8) was observed in the largest absorption peak. A smaller shift was observed in the λ = 548 nm peak (red shift to λ = 555 nm) and spectral distortion, with not much shift in the peak absorption, was seen at below $\lambda \sim 500$ nm. In contrast to the 1:1 UEDTA(aq) complex formation, isosbestic points were not clearly evident, indicating the likely coexistence of multiple species. Alteration of spectral patterns belonging to the UEDTA(aq) complex (*e.g.* at λ = 655 nm and λ = 674 nm) with increasing pH are in good agreement with Ermolaev and Krot, 1963,[12] who reported optical density results only at these two wavelengths. These authors suggested stepwise hydrolysis for the changes in the spectra and proposed the formation of $UEDTA(OH)^{-}$, $UEDTA(OH)_2^{2-}$, and $(UEDTAOH)_2^{2-}$. The same species, except for $UEDTA(OH)_2^{2-}$, are proposed by Carey et al., 1968[10] based on potentiometric experiments. The thermodynamic data derived in these studies were not selected by the NEA-TDB due to these discrepancies and the absence of well-defined pH measurements in Ermolaev and Krot, 1963.[12]

The spectral changes obtained with increasing pH are consistent with the stepwise hydrolysis reported in the literature, but the relative contribution of these species cannot be easily quantified based on their spectroscopy alone. The possible formation of oligomeric U(IV)-OH-EDTA complexes at pH ~ 4 was investigated the concentration of the complex to cover the range reported in the literature.[10] The absorption spectra of U(IV) as a function of $[U]_{tot}$ = $1.4 \cdot 10^{-4}$ M – $1.3 \cdot 10^{-3}$ M, at constant [U(IV)]:[EDTA] = 1:10 in 0.5 M NaCl at pH_m = 4 are shown in Figure S2a (supporting information). The UV–Vis–NIR measurements were performed with and without 10 kD filtration. No difference was observed between these absorption spectra indicating that > 2-3 nm colloidal species were not present. The spectra, when taken at various concentrations of the complex, showed no significant change in band shape (see Figure S2b), which suggested a predominance of the same speciation across the concentration range. These two observations do not agree with the previous work by Carey et al. (1968), who suggested the formation of the dimer $(UEDTAOH)_2^{2-}$ above $7.5 \cdot 10^{-4}$ M uranium concentrations.

In the variable-pH experiments, a yellow solid phase was formed at $pH_m > 2.5$ after 3 days of contact time. The precipitate observed differs from $UEDTA \cdot xH_2O(s)$ reported by Ermolaev and Krot, 1963,[12] in terms of its color (greyish green) and the apparent solubility ($6.45 \cdot 10^{-3}$ M). In order to check for the possible oxidation to U(VI) where solid phases frequently show yellow to orange color, a sample was prepared under the same experimental conditions at pH_m = 4 in 0.01M EDTA starting with $[U(VI)]_{tot}$ = 10^{-3} M but in the absence of Sn(II). A yellow phase started to precipitate within 3 days of contact time that would not occur in an EDTA-free system due to the higher solubility of $UO_3 \cdot H_2O(cr)$ at this pH. The aqueous and solid phases of these samples initially present as U(IV) or U(VI) were investigated by UV–Vis–NIR and XRD, respectively. Spectroscopically, changes were only observed in the UV–Vis–NIR spectrum of the sample that was initially U(VI) that indicated complete reduction to a U(IV)-EDTA complex. XRD analysis performed for both samples are shown in Figure S1 (supporting information). The same patterns were recorded for both solids, which did not match reference patterns reported for

UO_2(s), $UO_3 \cdot H_2O$(cr) or any the references in the XRD database.[27] Considering that a lower solubility that $UO_3 \cdot H_2O$(cr) was obtained, the solid phase formed was attributed to an unknown U-EDTA compound. UV–Vis–NIR and XRD results indicated that both samples, regardless of the starting oxidation state, reached the same aqueous speciation and solid phase after attaining steady-state conditions. Oxidation state analysis of this yellow solid phase is discussed in Section 3.3.

3.2 Undersaturation U(IV) solubility experiments in the presence of EDTA

Long-term undersaturation solubility studies were performed to establish the stability of the hydrolyzed UEDTA(aq) complexes and quantify their effect on the solubility of UO_2(s). The solubility of UO_2(s) in the presence of 0.01 M $[EDTA]_{tot}$ at pH_m = 4-11 in 0.5 and 5.0 M NaCl solutions are shown in Figure 2a and 2b, respectively. The concentration measurements from the oversaturation experiments as a function of pH_m discussed in Section 3.1 are also included in Figure 2a. The solubility measurements are compared with the calculated solubility of UO_2(am, hyd) in EDTA-free 0.5 and 5.0 M NaCl solutions based on the chemical, thermodynamic and activity data models summarized in Table S1 and Table S2. The undersaturation solubility samples were monitored up to 517 days, although steady-state conditions were attained within 2 weeks for the experiments at $pH_m \leq 10$. The experiment at $pH_m \sim 11$ in 0.5 M NaCl initially exhibited an apparent solubility that was about 2 orders of magnitude higher but the hydrolyzed EDTA complex was not stable with time. At longer times (239 days), the solubility had decreased to $[U] = 10^{-8}$ M in agreement with UO_2(am, hyd) solubility in equilibrium with $U(OH)_4$(aq).

All samples (except for $pH_m \approx 11$) showed a significant effect of EDTA on UO_2(s) solubility compared to the EDTA-free 0.5 and 5.0 M NaCl systems. At pH_m= 4-7, the measured concentrations were below saturation since complete dissolution of ~3 mg UO_2(s) was observed within 3 days. This prevented the evaluation of the number of H^+ involved in the solubility equilibrium in this pH_m-region. The absorption spectra recorded from these samples agreed very well with the spectra obtained in the oversaturation experiments, indicating the formation of U(IV)-OH-EDTA complexes (Figure S3, supporting information). In contrast with the oversaturation experiments, no yellow solid phase was formed. The concentration measurements at $pH_m > 7$ shows a steep decrease with increasing pH up to $pH_m = 11$. No significant difference was observed between the 0.5 and 5.0 M NaCl systems. This agreed with the Th(IV) solubility results obtained in the presence of 0.01 M EDTA in 0.5 and 6.0 M $NaNO_3$ reported[7]. XRD analysis (Figure S1, supporting information), performed after attaining equilibrium conditions, showed UO_2(s) as the solubility controlling solid phase at $pH_m > 7$ in both salt systems. There was no evidence of uranium oxidation or solid phase transformation over the course of the experiments.

The solubility calculations based on the NEA-TDB thermodynamic selection (which only included the formation of the UEDTA(aq) complex) defined a strong effect of EDTA on U(IV) solubility up to pH_m = 8 (Figure 2). The combined solubility and spectroscopic results obtained in the present study revealed the limitations of the current NEA-TDB selection: (i) The solubility measurements in the present study

above pH_m = 7 are significantly underestimated by the calculated solubility. (ii) The slope of the calculated solubility is steeper (slope = –4, corresponding to the equilibrium $UO_2(s) + 4H^+ + EDTA^{4-} \Leftrightarrow UEDTA(aq) + 2H_2O(l)$) than the slope in our solubility data at pH_m = 6–10 (≈ –2 to ≈ –3), indicated that a decreased number of protons are involved in the solubility equilibria. (iii) The absorbance measurements from both undersaturation and oversaturation experiments at pH_m 2.5 to 6.5 (See Figure 2 and Figure S3) reflected changes in the speciation with increasing pH. The further hydrolysis of the UEDTA(aq) complex, starting at pH_m ~ 2.5, is supported by all of these observations and the 1:1 UEDTA complex cannot be the only EDTA complex present up to pH_m = 8.

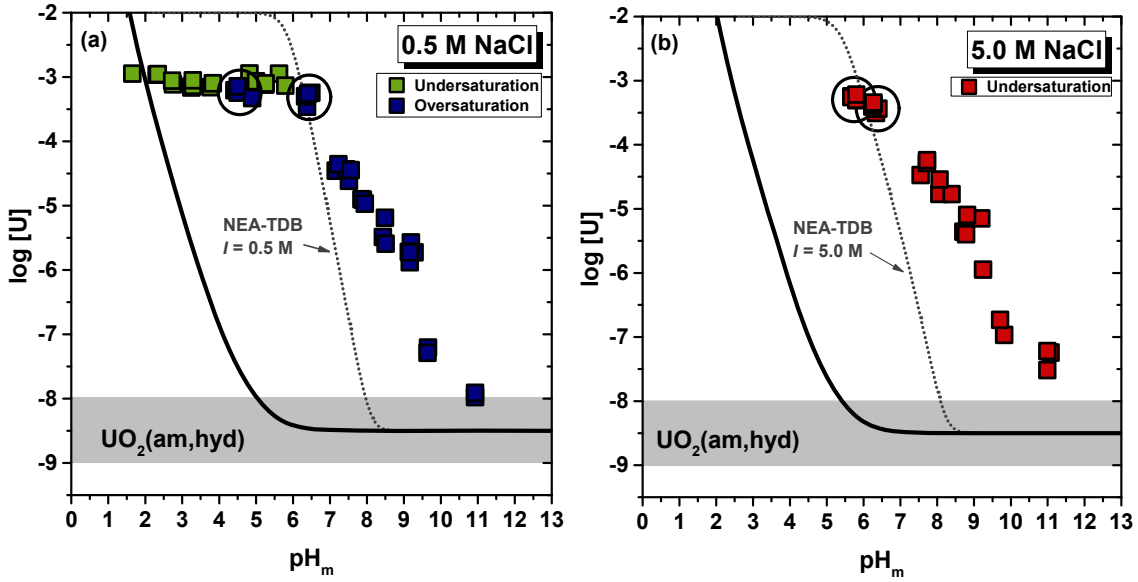

Figure 2 The solubility of $UO_2(s)$ in the presence of 0.01 M EDTA in the 0.5 M (a) and 5.0 M (b) NaCl systems. The solid line represents the solubility of UO_2(am, hyd) in the EDTA–free 0.5 and 5.0 M NaCl system calculated based on the data in Neck et al., 2001.[28] Circles indicate the undersaturation samples that were investigated by UV–Vis–NIR after attaining equilibrium conditions (Figure S3, supporting information).

The observations in the present study are consistent with the EDTA complexation behavior of the An(IV) series observed in the plutonium and thorium systems. The increase in solubility as well as the slope analysis agree with the observed Pu(IV) solubility trends in the presence of EDTA[3, 4]. Stepwise hydrolysis species, $PuEDTA(OH)^-$, $PuEDTA(OH)_2^{2-}$ and $PuEDTA(OH)_3^{3-}$ were used to explain the increase in PuO_2(am, hyd) solubility in the presence of EDTA at pH = 1.5-12. Similar results were reported for Th(IV)-EDTA systems[7] where the increase in ThO_2(am, hyd) solubility at pH_c = 5-12 was explained by the formation of $ThEDTA(OH)^-$, $ThEDTA(OH)_2^{2-}$ and $ThEDTA(OH)_3^{3-}$ species. The presence of dimeric $(ThEDTAOH)_2^{2-}$ species, which was previously reported by potentiometric titration

measurements[12], was not observed by EXAFS analysis even in the samples with high Th (0.03 M) and EDTA (0.1 M) concentrations. Based on the solubility and spectroscopic evidence in the present work and the strong analogy between the solution chemistry of actinides for given oxidation states,[28-31] it is concluded that U(IV) followed the same complexation trend as the other tetravalent actinides. It forms the UEDTA(aq) complex at $pH_m < 2.5$ and hydrolyzes with increasing pH according to reaction (1):

$$UO_2(am, hyd) + EDTA^{4-} + (4-x)\ H^+ \leftrightarrow UEDTA(OH)_x^{x-} + (2-x)\ H_2O(l) \quad (1)$$

3.3 Redox state analysis

3.3.1 Evaluation of reducing potential of the system

The redox conditions, in all but the pH_m ~1 experiments and the U(VI) study, were established by the added Sn(II) which was modified somewhat by the presence of EDTA. E_h measurements were made to evaluate this combined effect and link this to the observed behavior of the uranium systems investigated. pH_m and E_h (converted into pe) measurements of the investigated samples are shown in the Pourbaix diagram of U in the presence of EDTA (see Figure 3).

All evaluated experiments in the presence of EDTA at $pH_m < 7$ showed reducing conditions at $(pe + pH_m) = (6.5 \pm 1)$ regardless of the experimental approach (oversaturation *vs*. undersaturation) and the initial oxidation state of uranium. This contrasts with the lower reducing conditions reported for Sn(II)-buffered systems ($(pe + pH_m) = (2 \pm 1)$ in 0.5 M NaCl) in EDTA-free NaCl systems.[15, 16, 20] The difference observed between the $(pe + pH_m)$ measurements of Sn(II) in the presence and the absence of EDTA reflects the impact of this ligand on the Sn(II)/Sn(IV) redox distribution and accordingly, on the redox potential set by this couple. We hypothesize that the formation of strong Sn(II)-EDTA complexes, *i.e*., $SnEDTA^{2-}$, $SnHEDTA^-$ and $SnH_2EDTA(aq)$[32, 33], expanded the stability field of Sn(II), and thus decreased its effective reducing potential. The measured values $(pe + pH_m) = (6.5 \pm 1)$ are located very close to U(VI/IV) borderline based on current chemical and thermodynamic data, suggesting an equilibrium between both oxidations states of uranium. This disagreed with our spectroscopic measurements in this pH_m-range, which only showed the formation of U(IV)-EDTA complexes in the aqueous phase. Note that the consideration of U(IV)-OH-EDTA complexes in the thermodynamic calculations would result in a significant increase of the stability field of U(IV) in this pH_m-range, compared to the calculations shown in Figure 3. Stronger reducing conditions were measured in the samples at $pH_m > 7$, perhaps due to the absence or lesser prevalence of SnEDTA complexation. The $(pe + pH_m)$ values were (2 ± 1) at $pH_m > 8.5$, which was clearly below the U(VI/IV) borderline. This was more in line with the reducing conditions predicted for Sn(II)-buffered systems and also implied that U should be in the +IV redox state throughout these experiments.

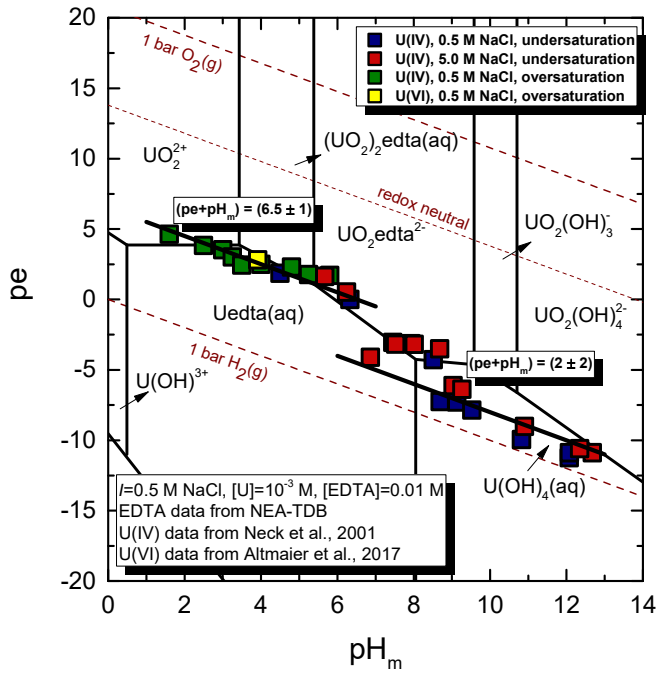

Figure 3 Pourbaix diagram of U in the presence of 0.01 M EDTA at I = 0.5 M NaCl calculated with the thermodynamic data given in Table S1 and Table S2. The black solid lines correspond to 50 : 50 distribution borderlines between aqueous U(VI) and U(IV) species. The dashed and dotted lines indicate upper and lower decomposition lines of water and "redox neutral" (pe + pH = 13.8), respectively.

3.3.2 XANES analysis

The U L_{III}-edge XANES spectra of selected samples, including reference spectra of U(VI) and U(IV) collected at the INE beamline[20], are shown in Figure 4. UV–Vis–NIR measurements of these samples are shown in Figure S4 (supporting information) and confirmed that the same aqueous U-EDTA species were successfully reproduced at KIT-INE. The experimental conditions and edge positions (white line, WL) are summarized in Table 2. No solid phase formation is observed in the oversaturation experiments that started with U(IV) at $pH_m \leq 6.5$. The edge positions of the aqueous samples in all investigated systems that were initiated with U(IV) are in excellent agreement with the position of the U(IV) reference (see Figure 4a and Table 2). These data confirmed that aqueous uranium is only found in the +IV redox state in the presence of EDTA. These results are also consistent with the absorbance measurements obtained by UV–Vis–NIR spectroscopy in the present work. The edge position of the solid sample at $pH_m \sim 9$ in 5.0 M NaCl was also confirmed as U(IV) in agreement with the presence of UO_2(s) as the solubility-controlling phase observed by XRD measurements (Figure S1, supporting information).

XANES spectra of both the supernatant and the yellow precipitate of the sample prepared with U(VI) at pH_m = 4 are shown in Figure 4b. The aqueous phase of this sample agrees very well with the edge positions of the U(IV) reference, indicating that reduction occurred. In contrast, the yellow precipitate showed a XANES spectra and edge position that was similar to the U(VI) reference samples. The same yellow solid phase was observed by XRD in both samples that started with U(IV) in Section 3.1 and U(VI) from oversaturation. This was not seen in the UO_2(s) undersaturation and U(IV) oversaturation experiments in KIT-INE, indicating that the noted shift to a higher redox potential did not lead to oxidation of U(IV). The fast precipitation was attributed to the presence of trace amount of U(VI) in the experiments in Section 3.1. The observations in the present study collectively indicate a strong effect of EDTA on both solubility and the redox behavior of uranium, which have not yet been reported. Thermodynamic calculations depicted on the Pourbaix diagram do not include hydrolyzed species of the U(IV)-EDTA complexes, nor the U(VI)-EDTA compounds. Although predictions based on E_h-pH measurements hint towards the possibility of mixed oxidation state equilibria around $pH_m \sim 4$, their speciation and predominance area could not be represented due to the lack of chemical, thermodynamic and activity models and the limitations of our data.

Table 2 XANES results of samples prepared at KIT-INE laboratories. Both the samples and the references are measured at the INE-Beamline.

Samples	**Edge position (eV)**
References	
Reference $UO_3 \cdot 2H_2O$(cr)	17179.4
Reference $Na_2U_2O_7 \cdot H_2O$(cr)	17179.9
Reference UO_2(s)	17176.6
Aqueous samples	
Oversat., $[U]^* = 1.3 \cdot 10^{-3}$ M, [EDTA] = 0.01 M, $I \sim 0.5$ M, at $pH_m \sim 0.3$	17176.7
Oversat., $[U]^* = 1.3 \cdot 10^{-3}$ M, [EDTA] = 0.01 M, $I \sim 0.5$ M, at $pH_m = 4.3$	17176.7
Oversat., $[U]^* = 1.3 \cdot 10^{-3}$ M, [EDTA] = 0.01 M, $I \sim 0.5$ M, at $pH_m = 6.5$	17176.6
Oversat., $[U]^* = 3.2 \cdot 10^{-4}$ M, [EDTA] = 0.01 M, $I = 0.5$ M, at $pH_m = 4.1$	17176.4
Solid samples	
Oversat., $[U]^* = 3.2 \cdot 10^{-4}$ M, [EDTA] = 0.01 M, $I = 0.5$ M, at $pH_m = 4.1$	17178.8
Undersat., $[U]^* = 1.1 \cdot 10^{-6}$ M, [EDTA] = 0.01 M, $I = 5.0$ M, at $pH_m = 9$	17176.8

*Measured uranium concentrations in solution after 6 months of equilibrium.

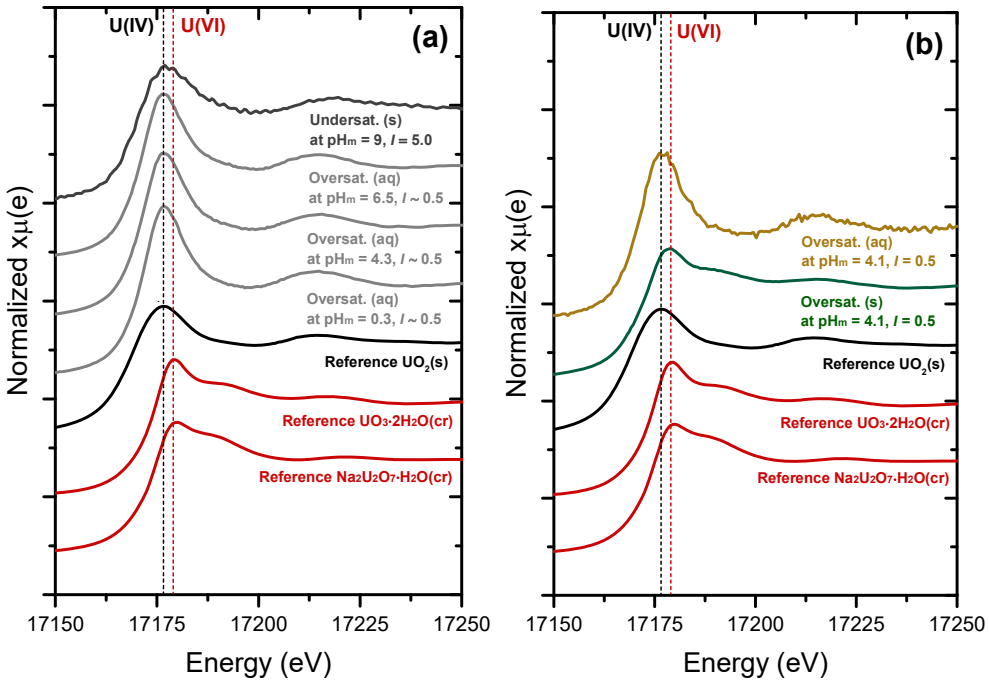

Figure 4 U L_{III} XANES spectra for the samples prepared at KIT-INE and summarized in Table 2. (a) aqueous and solid phase of the samples that started as U(IV), (b) aqueous and solid phase of the sample that started as U(VI). Red and black solid lines correspond to U(VI) and U(IV) references, respectively. Reference spectra were taken at the same beamline and reported in Çevirim-Papaioannou et al., (2018).[20]

4. Environmental aspects and summary

Reliable and comprehensive geochemical models are needed to predict and assess the potential migration of actinide contaminants from a nuclear waste repository or near-surface contaminated sites. Uranium and EDTA coexist as contaminants at a number of sites. They are also key waste components in transuranic or intermediate nuclear waste repository concepts (e.g., WIPP) where cleanup, reprocessing, and laboratory waste residue are comingled. It is important that the impact of EDTA on the speciation of uranium, and other An(IV) actinides, are understood for the range of environmentally-relevant conditions expected.

The results in the present work show that EDTA rapidly forms a strong complex with U(IV), and this complex is stable and undergoes further hydrolysis with increasing pH up to a pH_m ~ 10. These U(IV)-EDTA species significantly increase the solubility of UO_2(s) under environmentally and repository relevant neutral to alkaline pH conditions. EDTA can also impose and influence redox conditions in a way that affects the actinide speciation and, in our particular case, the speciation of uranium. In the absence of a redox-controlling additive, EDTA induced the reduction of U(VI) to U(IV) under anoxic conditions. In the presence of redox-impacting metals, EDTA may also alter the redox properties of a metal by forming a strong complex with the metal. In our case, there was a ~ 4.5 pe shift towards more

oxidizing conditions due to the Sn-EDTA complexation behavior. Lastly, there was a relatively small effect of ionic strength on the chemistry of the UEDTA systems investigated.

Collectively, the results in this study highlight a strong effect of EDTA on both the solubility and the oxidation-state distribution of uranium. This, by analogy, connects with and extends to all the An(IV) actinides. We also show that the uranium(IV) spectroscopy, although qualitatively insightful, cannot be readily used to quantify these changes in UEDTA speciation. This speciation is currently not modeled well in the Pourbaix diagrams calculated based on existing chemical and thermodynamic data. These calculations underestimate uranium(IV) solubility in the pH_m range (neutral to alkaline) that is most critical for environmental applications. Thermodynamic data for the solid phases and aqueous complexes of uranium observed are needed to properly describe the effects of EDTA for reliable long-term safety assessment calculations and source term estimations.

Acknowledgment

The authors would like to thank Dr. Juliet Swanson (LANL-ACRSP), Dr. Floyd E. Stanley (LANL-ACRSP), Dr. Joerg Rothe (KIT–INE), Dr. Nese Çevirim-Papaioannou (KIT–INE) and Mr. Frank Geyer (KIT–INE) for their technical support. This work was funded by the Department of Energy, Carlsbad Field Office as part of the WIPP project (Russ Patterson). Part of this work was funded by the German Ministry of Economic Affairs and Energy (BMWi) within the framework of the EDUKEM project with contract number 02E11334. We acknowledge the KIT light source for provision of instruments at the INE-Beamline operated by the Institute for Nuclear Waste Disposal and we would like to thank the Institute for Beam Physics and Technology (IBPT) for the operation of the storage ring, the Karlsruhe Research Accelerator (KARA).

References

1. Reed, D. T.; Borkowski, M.; Lucchini, J. F.; Richmann, M. K.; Garner, J. M. *Appendix SOTERM-2009: WIPP Actinide Chemistry Source Term*; LA-UR-13-24559; Los Alamos National Laboratory: 2013.

2. Riley, R. G.; Zachara, J. M. *Chemical Contaminants on DOE Land and Selection of Contaminant Mixtures for Subsurface Science Research*; 0031-3998; DOE/ER-0547T, U.S. Department of Energy, Office of Energy Research, Washington, DC.: 1992.

3. Rai, D.; Bolton, H.; Moore, D. A.; Hess, N. J.; Choppin, G. R., Thermodynamic model for the solubility of PuO_2(am) in the aqueous Na^+−H^+−OH^-−Cl^-−H_2O-ethylenediaminetetraacetate system. *Radiochim Acta* **2001,** *89*, 67.

4. Rai, D.; Moore, D. A.; Rosso, K. M.; Felmy, A. R.; Bolton, H., Environmental mobility of Pu(IV) in the presence of ethylenediaminetetraacetic acid: Myth or reality? *Journal of Solution Chemistry* **2008,** *37*, 957-986.

5. Rai, D.; Moore, D. A.; Felmy, A. R.; Rosso, K. M.; Bolton, H., $PuPO_4$(cr, hyd.) Solubility Product and Pu^{3+} Complexes with Phosphate and Ethylenediaminetetraacetic Acid. *Journal of Solution Chemistry* **2010,** *39*, 778-807.

6. Boukhalfa, H.; Reilly, S. D.; Smith, W. H.; Neu, M. P., EDTA and mixed-ligand complexes of tetravalent and trivalent plutonium. *Inorg Chem* **2004,** *43*, 5816-5823.

7. Xia, Y. X.; Felmy, A. R.; Rao, L. F.; Wang, Z. M.; Hess, N. J., Thermodynamic model for the solubility of ThO_2(am) in the aqueous Na^+-H^+-OH^--NO_3^--H_2O-EDTA system. *Radiochim Acta* **2003,** *91*, (12), 751-760.

8. Klygin, A. E.; Smirnova, I. D.; Nikol'skaya, N. A., The solubility of ethylenediaminetetraacetic acid in ammonia and hydrochloric acid and its reaction with uranium(IV) and plutonium(IV). *Russian Journal of Inorganic Chemistry* **1959,** *4*, 1279-1282.

9. Krot, N. N.; Ermolaev, N. P.; Gel'man, A. D., The behaviour of ethylenediaminetetraacetic acid in acid solutions and its reaction with uranium(IV). *Russian Journal of Inorganic Chemistry* **1962,** *7*, 1062-1066.

10. Carey, G. H.; Martell, A. E., Formation, hydrolysis, and olation of uranium(IV) chelates. *Journal of American Chemical Society* **1968,** *90*, 32-38.

11. Hummel, W.; Anderegg, G.; Rao, L.; Puigdomenech, I.; Tochiyama, O., *Chemical thermodynamics of compounds and complexes of U, Np, Pu, Am, Tc, Se, Ni and Zr with selected organic ligands*. Elsevier: Issy-les-Moulineaux, France, 2005; Vol. 9.

12. Ermolaev, N. P.; Krot, N. N., Complex formation between uranium(IV) and ethylenediaminetetraacetic acid. *Russian Journal of Inorganic Chemistry* **1963,** *8*, 1282-1289.

13. Thein, S. M.; Bereolos, P. J. *Thermal Stabilization of UO_2, UO_3 and U_3O_8*; ORNL/TM-2000/82; Oak Ridge National Laboratory: 2000.

14. Altmaier, M.; Metz, V.; Neck, V.; Muller, R.; Fanghänel, T., Solid-liquid equilibria of $Mg(OH)_2$(cr) and $Mg_2(OH)_3Cl.4H_2O$(cr) in the system Mg-Na-H-OH-O-Cl-H_2O at 25ºC. *Geochim Cosmochim Ac* **2003,** *67*, (19), 3595-3601.

15. Kobayashi, T.; Scheinost, A. C.; Fellhauer, D.; Gaona, X.; Altmaier, M., Redox behavior of Tc(VII)/Tc(IV) under various reducing conditions in 0.1 M NaCl solutions. *Radiochim Acta* **2013,** *101*, (5), 323-332.

16. Yalcintas, E.; Gaona, X.; Scheinost, A. C.; Kobayashi, T.; Altmaier, M.; Geckeis, H., Redox chemistry of Tc(VII)/Tc(IV) in dilute to concentrated NaCl and $MgCl_2$ solutions. *Radiochim Acta* **2015,** *103*, (1), 57-72.

17. Puigdoménech, P. *INPUT, SED and PREDOM: Computer Programs Drawing Equilibrium Diagrams, TRITA-OOK-3010*; 0094-2405; Royal Institute of Technology (KTH), Dept. Inorg. Chemistry, Stockholm (Sweden): Dec, 1983.

18. Rothe, J.; Butorin, S.; Dardenne, K.; Denecke, M. A.; Kienzler, B.; Loble, M.; Metz, V.; Seibert, A.; Steppert, M.; Vitova, T.; Walther, C.; Geckeis, H., The INE-Beamline for actinide science at ANKA. *Review of Scientific Instruments* **2012,** *83*, (4).

19. Zimina, A.; Dardenne, K.; Denecke, M. A.; Doronkin, D. E.; Huttel, E.; Lichtenberg, H.; Mangold, S.; Pruessman, T.; Rothe, J.; Spangenberg, T.; Steininger, R.; Vitova, T.; Geckeis, H.; Grunwaldt, J. D., CAT-ACT—A new highly versatile x-ray spectroscopy beamline for catalysis and radionuclide science at the KIT synchrotron light facility ANKA *Review of Scientific Instruments* **2017,** *88*, 113113.

20. Çevirim-Papaioannou, N.; Yalcintas, E.; Gaona, X.; Dardenne, K.; Altmaier, M.; Geckeis, H., Redox chemistry of uranium in reducing, dilute to concentrated NaCl solutions. *Applied Geochemistry* **2018,** *98*, 286-300.

21. Tasi, A.; Gaona, X.; Fellhauer, D.; Bottle, M.; Rothe, J.; Dardenne, K.; Schild, D.; Grive, M.; Colas, E.; Bruno, B.; Kallstrom, K.; Altmaier, M.; Geckeis, H., Redox behavior and solubility of plutonium under alkaline, reducing conditions. *Radiochim Acta* **2018,** *106(4)*, 259-279.

22. Yalcintas, E.; Gaona, X.; Altmaier, M.; Dardenne, K.; Polly, R.; Geckeis, H., Thermodynamic description of Tc(IV) solubility and hydrolysis in dilute to concentrated NaCl, $MgCl_2$ and $CaCl_2$ solutions. *Dalton Transactions* **2016,** *45*, 8916-8936.

23. Gaona, X.; Tits, J.; Dardenne, K.; Liu, X.; Rothe, J.; Denecke, M. A.; Wieland, E.; Altmaier, M., Spectroscopic investigations of Np(V/VI) redox speciation in hyperalkaline TMA-(OH, Cl) solutions. *Radiochim. Acta* **2012,** *100*, 759-770.

24. Finck, N.; Dardenne, K., Interaction of selenite with reduced Fe and/or S species: An XRD and XAS study. *Journal of Contaminant Hydrology* **2016,** *188*, 44-51.

25. Ravel, B.; Newville, M., ATHENA, ARTEMIS, HEPHAESTUS: data analysis for X-ray absorption spectroscopy using IFEFFIT. *J. Synchrotron Radiat.* **2005,** *12*, 537-541.

26. Cohen, D.; Carnall, W. T., Absorption spectra of uranium(III) and uranium(IV) in $DClO_4$ solution. *Journal of Physical Chemistry* **1960,** *64*, 1933-1936.

27. JCPDS, Powder diffraction files. Joint Committee on Powder Diffraction Standards. Swarthmore. In USA (2001), 2001.

28. Neck, V.; Kim, J. I., Solubility and hydrolysis of tetravalent actinides. *Radiochim. Acta* **2001,** *89*, (1), 1-16.

29. Neck, V.; Altmaier, M.; Rabung, T.; Lutzenkirchen, J.; Fanghanel, T., Thermodynamics of trivalent actinides and neodymium in NaCl, MgCl2, and CaCl2 solutions: Solubility, hydrolysis, and ternary Ca-M(III)-OH complexes. *Pure Appl Chem* **2009,** *81*, (9), 1555-1568.

30. Altmaier, M.; Neck, V.; Fanghanel, T., Solubility of Zr(IV), Th(IV) and Pu(IV) hydrous oxides in $CaCl_2$ solutions and the formation of ternary Ca-M(IV)-OH complexes. *Radiochim Acta* **2008,** *96*, (9-11), 541-550.

31. Fellhauer, D.; Neck, V.; Altmaier, M.; Lutzenkirchen, J.; Fanghanel, T., Solubility of tetravalent actinides in alkaline $CaCl_2$ solutions and formation of $Ca_4[An(OH)_8]^{4+}$ complexes: A study of Np(IV) and Pu(IV) under reducing conditions and the systematic trend in the An(IV) series. *Radiochim Acta* **2010,** *98*, (9-11), 541-548.

32. Langer, H. G.; Bogucki, R. F., The chemistry of tin(II) chelates-II. *J. inorg, nucl. Chem* **1967,** *29*, 495-402.

33. Bottari, E.; Liberti, A.; Rufolo, A., Potentiometric investigation of complexes between tin(II) and edta. *J. inorg, nucl. Chem* **1967,** *30*, 2173-2179.

34. Guillaumont, R.; Fanghänel, T.; Neck, V.; Fuger, J.; Palmer, D. A.; Grenthe, I.; Rand, M. H., *Update on the chemical thermodynamics of uranium, neptunium, plutonium, americium and technetium*. Elsevier: North-Holland, Amsterdam, 2003; Vol. 5.

35. Altmaier, M.; Yalcintas, E.; Gaona, X.; Volker, N.; Müller, R.; Schlieker, M.; Fanghänel, T., Solubility of U(VI) in chloride solutions. I. The stable oxides/hydroxides in NaCl systems, solubility products, hydrolysis constants and SIT coefficients. *Journal of Chemical Thermodynamics* **2017,** *114*, 2-13.

36. Grenthe, I.; Puigdoménech, I., *Modelling in Aquatic Chemistry*. OECD Nuclear Energy Agency Paris, 1997.

Supporting Information

Table S1 Equilibrium constants for the solubility, hydrolysis and EDTA complexation reactions of uranium considered for thermodynamic calculations in the present study.

Reactions	log*K°	Reference
Redox		
$UO_2^{2+} + 4H^+ + 2e^- \leftrightarrow U^{4+} + 2H_2O$	(9.04 ± 0.04)	Guillaumont et al. (2003)[34]
$UO_2^{2+} + e^- \leftrightarrow UO_2^+$	(1.49 ± 0.02)	Guillaumont et al. (2003)[34]
$U^{4+} + e^- \leftrightarrow U^{3+}$	– (9.353 ± 0.07)	Guillaumont et al. (2003)[34]
Solubility		
UO_2(am, hyd) + $4H^+ \leftrightarrow U^{4+} + 4H_2O$	(1.50 ± 1.00)	Guillaumont et al. (2003)[34]
$UO_3{\cdot}2H_2O$(cr) + $2H^+ \leftrightarrow UO_2^{2+} + 3H_2O$	(5.35 ± 0.13)	Altmaier et al. (2017)[35]
$0.5Na_2U_2O_7{\cdot}H_2O$(cr) + $3H^+ \leftrightarrow Na^+ + UO_2^{2+}$	(12.20 ± 0.20)	Altmaier et al. (2017)[35]
U(IV) hydrolysis and complexation		
$U^{4+} + H_2O(l) \leftrightarrow UOH^{3+} + H^+$	–(0.40 ± 0.20)	Neck et al. (2001)[28]
$U^{4+} + 2H_2O(l) \leftrightarrow U(OH)_2^{2+} + 2H^+$	–(1.10 ± 1.00)	Neck et al. (2001)[28]
$U^{4+} + 3H_2O(l) \leftrightarrow U(OH)_3^+ + 3\ H^+$	–(4.70 ± 1.00)	Neck et al. (2001)[28]
$U^{4+} + 4H_2O(l) \leftrightarrow U(OH)_4(aq) + 4H^+$	–(10.00 ± 1.40)	Neck et al. (2001)[28]; Guillaumont et al.
$U^{4+} + EDTA^{4-} \leftrightarrow UEDTA(aq)$	(29.5 ± 0.2)*	Hummel et al. (2005)[11]
U(VI) hydrolysis and complexation		
$UO_2^{2+} + H_2O(l) \leftrightarrow UO_2OH^+ + H^+$	–(5.25 ± 0.24)	Guillaumont et al. (2003)[34]
$UO_2^{2+} + 2H_2O(l) \leftrightarrow UO_2(OH)_2(aq) + 2H^+$	–(12.15 ± 0.17)	Guillaumont et al. (2003)[34]
$UO_2^{2+} + 3H_2O(l) \leftrightarrow UO_2(OH)_3^- + 3H^+$	–(20.70 ± 0.42)	Altmaier et al. (2017)[35]
$UO_2^{2+} + 4H_2O(l) \leftrightarrow UO_2(OH)_4^{2-} + 4H^+$	–(31.90 ± 0.33)	Altmaier et al. (2017)[35]
$2UO_2^{2+} + H_2O(l) \leftrightarrow (UO_2)_2OH^{3+} + H^+$	–(2.70 ± 1.00)	Guillaumont et al. (2003)[34]
$2UO_2^{2+} + 2H_2O(l) \leftrightarrow (UO_2)_2(OH)_2^{2+} + 2H^+$	–(5.62 ± 0.06)	Guillaumont et al. (2003)[34]
$3UO_2^{2+} + 4H_2O(l) \leftrightarrow (UO_2)_3(OH)_4^{2+} + 4H^+$	–(11.90 ± 0.30)	Guillaumont et al. (2003)[34]
$3UO_2^{2+} + 5H_2O(l) \leftrightarrow (UO_2)_3(OH)_5^+ + 4H^+$	–(15.55 ± 0.12)	Guillaumont et al. (2003)[34]
$3UO_2^{2+} + 7H_2O(l) \leftrightarrow (UO_2)_3(OH)_7^- + 7H^+$	–(32.20 ± 0.80)	Guillaumont et al. (2003)[34]
$4UO_2^{2+} + 7H_2O(l) \leftrightarrow (UO_2)_4(OH)_7^+ + 7H^+$	–(21.90 ± 1.00)	Guillaumont et al. (2003)[34]
$UO_2^{2+} + EDTA^{4-} \leftrightarrow UO_2EDTA^{2-}$	(13.7 ± 0.2)	Hummel et al. (2005)[11]
$2UO_2^{2+} + EDTA^{4-} \leftrightarrow (UO_2)_2EDTA(aq)$	(20.6 ± 0.4)	Hummel et al. (2005)[11]
$UO_2^{2+} + HEDTA^{3-} \leftrightarrow UO_2(HEDTA)^-$	(8.37 ± 0.1)	Hummel et al. (2005)[11]

*Recalculated based on the experimental data in Krot and Ermaloev, 1962[9] and Carey et al., 1968[10]

Table S2 SIT ion interaction coefficients (in kg·mol^{-1}) of U(IV), U(V) and U(VI) species in NaCl solutions at 25°C considered for activity corrections in the present study.

i	*j*	*ε(i,j)*	Reference
U(IV) species			
U^{4+}	Cl^-	(0.36 ± 0.10)	Neck et al. (2001)[28]
$U(OH)^{3+}$	Cl^-	(0.20 ± 0.10)	Neck et al. (2001)[28]
$U(OH)_2^{2+}$	Cl^-	(0.10 ± 0.10)	Neck et al. (2001)[28]
$U(OH)_3^+$	Cl^-	(0.05 ±0.10)	Neck et al. (2001)[28]
$U(OH)_4$(aq)	Na^+, Cl^-	0[a]	Grenthe and Puigdoménech [36]
UEDTA(aq)	Na^+, Cl^-	0[a]	Grenthe and Puigdoménech [36]
U(V) species			
UO_2^+	Cl^-	(0.09 ± 0.05)[b]	Guillaumont et al. (2003)[34]
U(VI) species			
UO_2^{2+}	Cl^-	(0.21 ± 0.02)	Altmaier et al. (2017)[35]
$UO_2(OH)^+$	Cl^-	(0.10 ± 0.10)	Altmaier et al. (2017)[35]
$UO_2(OH)_2$(aq)	Na^+, Cl^-	0[a]	Grenthe and Puigdoménech [36]
$UO_2(OH)_3^-$	Na^+	–(0.24 ± 0.09)	Altmaier et al. (2017)[35]
$UO_2(OH)_4^{2-}$	Na^+	(0.01 ± 0.04)	Altmaier et al. (2017)[35]
$(UO_2)_2(OH)_2^{2+}$	Cl^-	(0.30 ± 0.06)	Altmaier et al. (2017)[35]
$(UO_2)_3(OH)_4^{2+}$	Cl^-	–(0.07 ± 0.17)	Altmaier et al. (2017)[35]
$(UO_2)_3(OH)_5^+$	Cl^-	(0.24 ± 0.15)	Altmaier et al. (2017)[35]
$(UO_2)_3(OH)_7^-$	Na^+	–(0.24 ± 0.09)	Altmaier et al. (2017)[35]
$(UO_2)_4(OH)_7^+$	Cl^-	(0.17 ± 0.18)	Altmaier et al. (2017)[35]
UO_2EDTA^{2-}	Na^+	– (0.22 ± 0.18)	Hummel et al. (2005)[11]
$(UO_2)_2$EDTA(aq)	Na^+, Cl^-	0[a]	Grenthe and Puigdoménech [36]
$UO_2(HEDTA)^-$	Na^+	– (0.18 ± 0.16)	Hummel et al. (2005)[11]

a. by definition in SIT; b. estimated considering $\varepsilon(UO_2^+, Cl^-) = 0.38 \cdot \varepsilon(UO_2^+, ClO_4^-)$

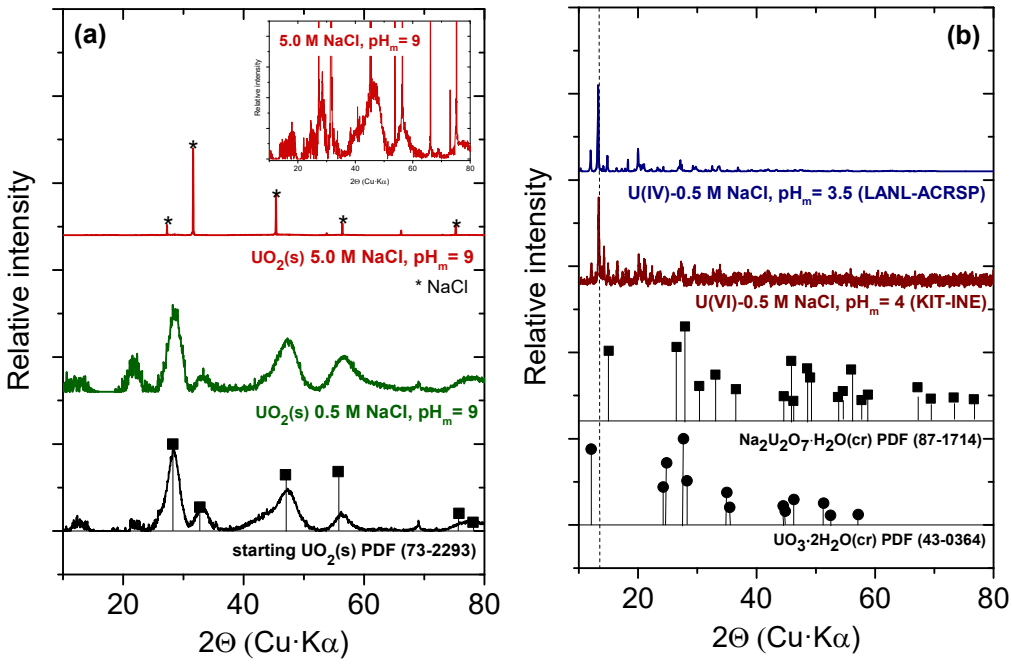

Figure S1 XRD diffractograms of undersaturation U(IV) samples (a) and the yellow precipitates formed in the U(IV) and U(VI) samples (b).

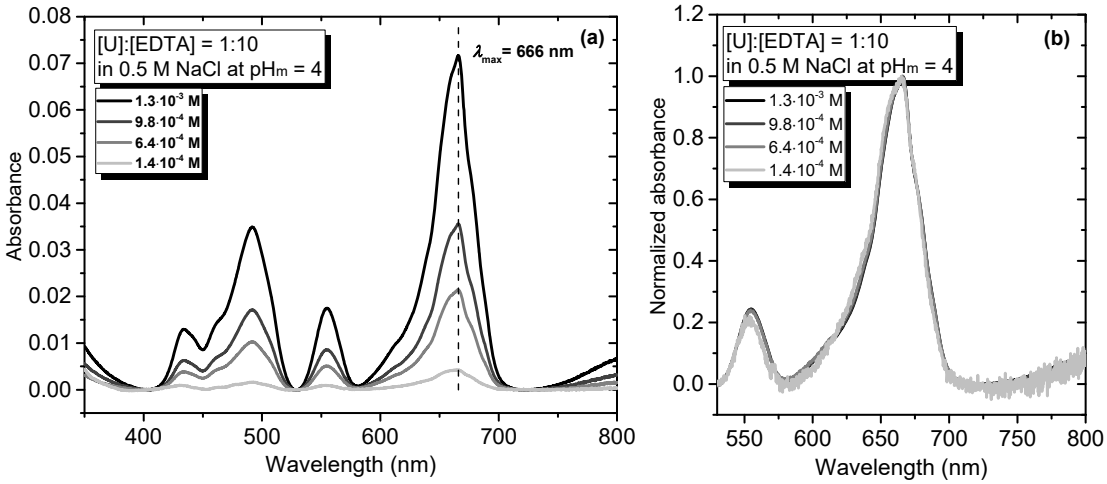

Figure S2 Absorption spectra (a) and normalized absorbance (b) of the U-EDTA complexes as a function of complex concentration from $1.4 \cdot 10^{-4}$ M to $1.3 \cdot 10^{-3}$ M at $pH_m = 4$ in 0.5 M NaCl.

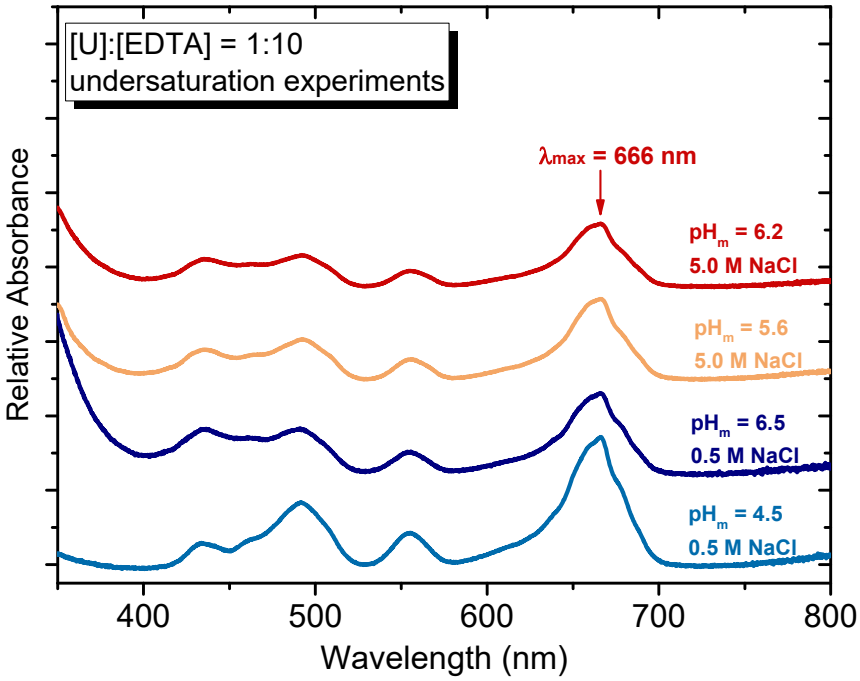

Figure S3 Absorption spectra of the UO_2(s) solubility samples with [U(IV)] > 10^{-4} M in the presence of 0.01 M EDTA in 0.5 and 5.0 M NaCl solutions.

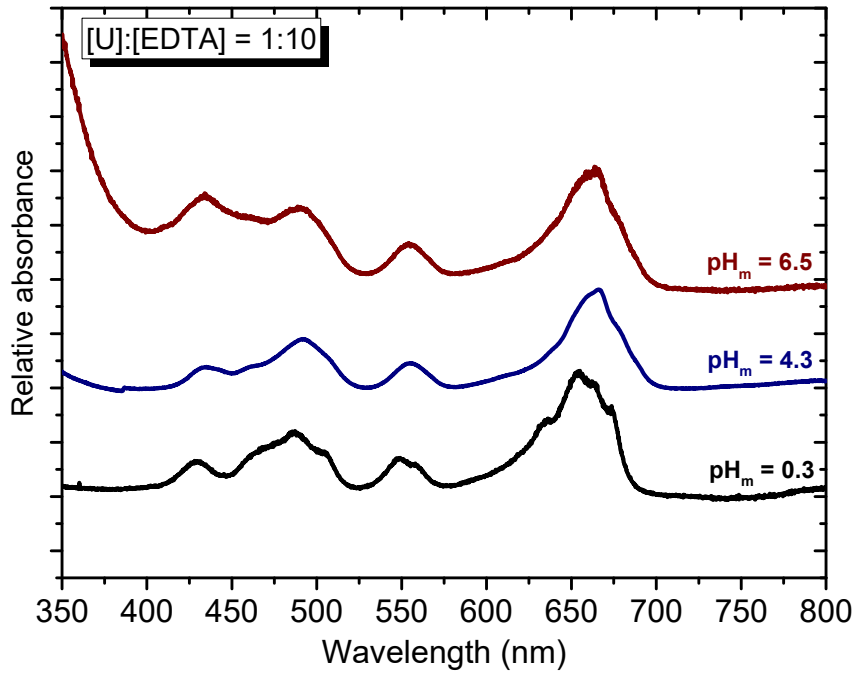

Figure S4 Absorption spectra of U-EDTA complexes reproduced in KIT-INE laboratories. Measurements are recorded prior to XANES analysis.